Shape transition during nest digging in ants

Etienne Toffin[a,1], David Di Paolo[a], Alexandre Campo[b], Claire Detrain[a], and Jean-Louis Deneubourg[a]

[a]Service d'Écologie Sociale, CP231, Université Libre de Bruxelles, Plaine Campus, Boulevard du Triomphe, 1050 Brussels, Belgium; and [b]Institut de Recherches Interdisciplinaires et de Développement en Intelligence Artificielle, Computer and Decision Engineering, CP194/6, Université Libre de Bruxelles, 50 Avenue Franklin Roosevelt, 1050 Brussels, Belgium

Nest building in social insects is among the collective processes that show highly conservative features such as basic modules (chambers and galleries) or homeostatic properties. Although ant nests share common characteristics, they exhibit a high structural variability, of which morphogenesis and underlying mechanisms remain largely unknown. We conducted two-dimensional nest-digging experiments under homogeneous laboratory conditions to investigate the shape diversity that emerges only from digging dynamics and without the influence of any environmental heterogeneity. These experiments revealed that, during the excavation, a morphological transition occurs because the primary circular cavity evolves into a ramified structure through a branching process. Such a transition is observed, whatever the number of ants involved, but occurs more frequently for a larger number of workers. A stochastic model highlights the central role of density effects in shape transition. These results indicate that nest digging shares similar properties with various physical, chemical, and biological systems. Moreover, our model of morphogenesis provides an explanatory framework for shape transitions in decentralized growing structures in group-living animals.

self-organization | nest building | branching pattern | modeling | collective behavior

The building of structures by animals is a widely spread phenomenon, from protozoa to primates (1). These structures can be considered an extension of the animal body: They have an adaptive value by improving the regulation of energetic exchanges with the outer environment (2), by ensuring the management of waste compounds (3), and by allowing food storage or protection against predation, but also by shaping the spatial distribution of social interactions (4). The nests of social insects take over all of these functions and show a robust relationship between nest volume and colony size (5–9). In ants, every nest is made of the same basic building modules (9–11) (i.e. chambers, tunnels), the sameness of which contrasts with the diversity of nest architecture (number and proportion of different modules, nest topology, and pattern regularity) that varies not only interspecifically but also intraspecifically according to the colony growth process (7, 9).

Although a dynamic study of nest building is essential to understand how the diversity of patterns is generated, there are few such studies (5, 6) addressing this issue. Most research describes final nest structures (7, 9, 12) or focuses on particular digging behaviors (13, 14) but provides few insights on the building process as a whole or on the mechanisms that generate a diversity of nest shapes.

The prevailing questions, therefore, are: Does the shape diversity find its origin in the complexity of the building behaviors of the insects, a specific behavior being associated to a specific shape or in quantitative changes in digging activity? Does it result from changes in the insect environment due to the building process itself? Or does the nest pattern emerge under strict control of the environment? Undoubtedly, all these parameters and behaviors should not be considered as alternatives: They interact constantly with one another and influence the building process at different levels.

In order to set apart the influence of environmental heterogeneities on the diversity of nest shapes, our experiments on

Lasius niger ants were conducted by using a two-dimensional (2D)-homogeneous setup. Such a study is required to understand how, and to what extent, morphogenesis relies on the digging dynamics and the influence of the excavated structure on the building behavior. Furthermore, as the colony size is known to regulate the digging activity (5, 8), we compared two experimental conditions (groups of 50 and 300 workers) to assess the influence of group size on morphogenesis as well as on shape transition during the building process.

Results

Excavation Dynamics. Our results show that the nest excavation begins with fast and amplified growth and reaches a saturation phase at which activity almost totally ceases (Fig. 1*A*), as highlighted in previous works (5, 8). We fit this digging dynamics with the following equation:

$$A = \frac{A_M t^\alpha}{\beta^\alpha + t^\alpha},$$ [1]

where A (in cm^2) is the excavated area (i.e. the nest area), t (in hours) is the time elapsed since the start of nest digging, A_M is the maximal area of the nest that is ultimately dug out, α stands for the cooperation level between ants (300 ants: $\alpha = 1.72 \pm 0.33$, $n = 33$; 50 ants: $\alpha = 1.38 \pm 0.33$, $n = 20$) and β is the time value when $A = 0.5 A_M$ (i.e. when half of the maximal nest area has been excavated; 300 ants: $\beta = 8.84 \pm 3.84$ h, $n = 33$; 50 ants: $\beta = 12.17 \pm 5.37$ h, $n = 20$) (fitting with Eq. **1** always returned coefficient of determination $r^2 \geq 0.95$). High α and low β values characterize a high and fast digging activity that is enhanced in large groups of ants. During the experiment, the digging rate (R), calculated as the derivative $\frac{dA}{dt}$ of the fitted area from Eq. **1**, reaches a maximum and decreases until it ceases, or tends to be residual when $A \simeq A_M$.

Morphological Growth. The most striking result of our experiments is the occurrence of a sharp morphological transition (Fig. 2; see also Movies S1 and S2 of the *SI Appendix*) that separates two distinct growth stages. The morphological transition occurs when the nest excavation goes from a first stage of circular and isotropic growth (Fig. 2*A*) to a second one of ramified growth (Fig. 2 *B–C*). During this second stage, characterized by a branching pattern, small buds appear regularly along the wall of the nest, some of them growing into lateral galleries. We note that because the environment is identical throughout the experimental arena, this transition must be purely a result of the internal dynamics.

The relationship between nest area (A) and nest perimeter (P) ($P = \mu A^\omega$) characterizes the nest morphology, and its variation
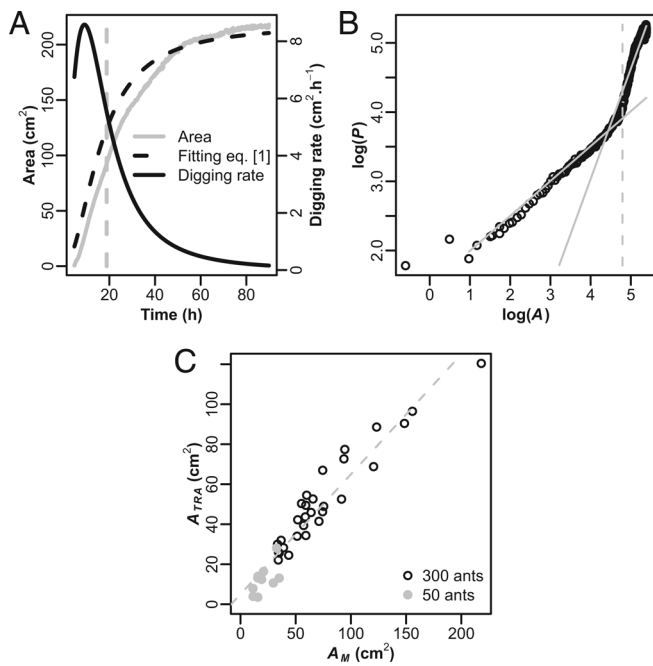
Fig. 1. Quantitative characterization of morphological transition. (*A* and *B*) Example of experimental results (experiment 30). The gray dashed vertical line corresponds to the occurrence of the morphological transition, which separates the first and second growth stages. (*A*) Evolution of the nest area and digging rate (Eq. **1** fitting parameters: $A_M = 218.10$ cm^2; $\alpha = 1.95$; $\beta = 16.3$ h; $r^2 = 0.99$). The gray line represents the area, the black dashed line corresponds to the Eq. **1** fitting curve, and the black curve represents the digging rate. The digging rate is calculated as the derivative $\frac{dA}{dt}$ of the fitted area from Eq. **1**. (*B*) Logarithm of the perimeter ($log(P)$) versus logarithm of the area ($log(A)$) of the nest. Gray lines correspond to the linear fits for the first and second stages with slope ω (respectively $\omega = 0.50$ and $\omega = 1.60$). (*C*) The relation between nest areas at transition (A_{TRA}) and at the end of experiments (A_M) for both group size (black open circles: 300 ants, $n = 29$; gray open circles: 50 ants, $n = 12$) ($A_{TRA} = 0.60 * A_M + 5.06$, $F_{1,39} = 446$, $P < 0.0001$, $r^2 = 0.92$).

through time allows us to identify the occurrence of such morphological transition (see *Materials and Methods*). During the first stage, where activity rate is the highest, the nest cavity can be roughly approximated by a growing disc with a smooth and regular wall. The value of ω during this stage (300 ants: $\omega_1 = 0.50 \pm 0.03$, $n = 29$; 50 ants: $\omega_1 = 0.56 \pm 0.05$, $n = 12$) (Fig. 1*B* and Table 1) confirms that the nest is close to a regular disc ($\omega = 0.5$). When the nest area A reaches a critical value (A_{TRA}), several buds appear along the nest wall and make the perimeter increase longer abruptly than the area, the nest shape being no longer like a disc. The relationship between A and P, therefore, changes sharply, as evidenced by the high values of ω (300 ants: $\omega_2 = 1.84 \pm 0.83$, $n = 29$; 50 ants: $\omega_2 = 1.55 \pm 0.62$, $n = 12$). In some cases, no

transition occurred. These experiments are characterized during the whole digging process by a ω value close to 0.5 (300 ants: $\omega_1 = 0.49 \pm 0.03$, $n = 4$; 50 ants: $\omega_1 = 0.61 \pm 0.10$, $n = 8$), meaning that nests dug remained smooth and round.

The main difference between the two experimental conditions lies in the number of experiments showing no transition from a circular to a ramified nest: 40% for 50 ants ($n = 20$ experiments) against 12% for 300 ants ($n = 33$ experiments). Furthermore, values of the estimated area dug per ant ($A_{M\text{NORM}}$, Table 1) are lower for large group size, which supports a rule previously shown in several studies (5–8), according to which the nest area increases sublinearly with the group size.

The larger the group size, the higher the transition (A_{TRA}) and ultimate (A_M) area values (Table 1). The transition occurs when the nest area has reached 60% of its final value A_M whatever the group size (Fig. 1*C* and Table 1). Within the same group size (50 or 300 ants), A_{TRA} and A_M vary between experiments (Table 1). This variance is probably due to differences in the activity level of tested groups of ants that can also be increased by amplification processes (15, 16). The larger the group and the more active the ants, the more workers dig (A_M) and the later (greater A_{TRA}) the morphological transition occurs.

Experiments without transition are characterized by lower ultimate nest areas (A_M) that are similar to area values of transition (A_{TRA}) of ramified nests (experiments without transition = 300 ants: $A_M = 53.81 \pm 20.35$ cm^2, $n = 4$; 50 ants: $A_M = 11.95 \pm 4.25$ cm^2, $n = 8$), suggesting that a threshold of mean digging activity and/or of excavated area must be reached in order to observe a change in the nest shape.

Combining the global digging activity (approximated by the digging rate R) and the cavity area (A) at any time of the experiment, we define the density of activity (ρ),

$$\rho = \frac{R}{A}, \qquad \qquad [2]$$

which should not be confused with density of individuals. The density of activity decreases from the beginning of the experiment until its end (Table 1). Despite the high variability of densities of activity during the first stage, the morphological transition is characterized by a value of ρ (ρ_{TRA}) independent of group size (300 ants: $\rho_{TRA} = 0.038 \pm 0.022$ h^{-1}, $n = 29$; 50 ants: $\rho_{TRA} = 0.041 \pm 0.045$ h^{-1}, $n = 12$) (see Table 1).

Simulations. Based on these results, we propose a scenario to explain the morphological transition in nest shape. We assume that the nest area is a limiting factor of the digging activity, because crowding close to the digging front and/or limitation of the worker traffic between the front and the unloading zone of excavated material may occur depending on nest size (see Fig. S1 of the *SI Appendix*). At the start of nest excavation, the digging behavior of ants is stimulated and amplified by different processes, such as pheromone release (17), interattraction between workers (18),
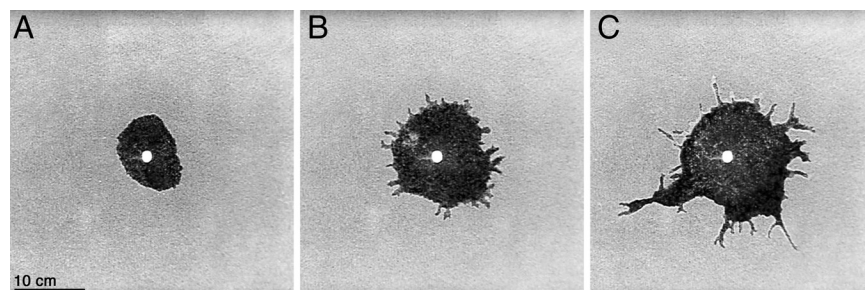
Fig. 2. Morphological transition occurring during nest digging in ants. (*A–C*) Snapshots of the nest showing the two successive digging stages (experiment 30). (*A*) First stage of homogeneous and circular digging. (*B* and *C*) Second stage where buds appear over the nest wall, some of them growing into lateral galleries through a branching process.

PHYSICS

ECOLOGY

Table 1. Comparison between 300- and 50-ant experiments with a morphological transition

Feature	Parameter	Mean ± SD (number of replicates)		Mann–Whitney test	
		300 ants	50 ants	U statistics	P value
Dynamic	α	1.71 ± 0.34 (29)	1.39 ± 0.33 (12)	72	0.003
	β	9.16 ± 4.00 (29)	12.61 ± 5.76 (12)	245	0.042
	A_M	75.18 ± 42.76 (29)	20.18 ± 7.99 (12)		
	$A_{M\text{Norm}}$	**0.251 ± 0.143 (29)**	**0.404 ± 0.160 (12)**	61	<0.001
Transition	ω_1	0.50 ± 0.03 (29)	0.56 ± 0.05 (12)	291	<0.001
	ω_2	1.84 ± 0.83 (29)	1.55 ± 0.62 (12)	132	0.238
	A_{Tra}	51.99 ± 24.41 (29)	12.60 ± 6.35 (12)		
	A_{TraNorm}	**0.173 ± 0.081 (29)**	**0.252 ± 0.127 (12)**	**92**	**0.018**
Density*	P_{Tra}	36.47 ± 11.98 (29)	21.85 ± 8.71 (12)		
	ρ_M	0.535 ± 0.390 (29)	0.758 ± 0.908 (12)	148	0.470
	ρ_{75}	0.291 ± 0.170 (29)	0.388 ± 0.448 (12)	155	0.601
	ρ_{50}	0.066 ± 0.029 (29)	0.072 ± 0.050 (12)	187	0.724
	ρ_{Tra}	0.038 ± 0.022 (29)	0.041 ± 0.045 (12)	202	0.436

Boldface font values have been normalized before statistical comparison (see *Materials and Methods*).
*Reference densities corresponding to specific values of digging rate are calculated chronologically: ρ_M when rate is maximum ($R = R_M$), ρ_{75} when $R = 0.75R_M$, ρ_{50} when $R = 0.50R_M$ and ρ_{Tra} at the transition time.

and/or activity by-product (14, 19). Then the group of digging ants quickly reaches a maximal value of potentially active workers. As the number of digging ants stays large (relatively to nest area and perimeter), workers cannot perform localized digging because of the crowding of ants along the perimeter of the nest. However, as the nest area increases, the average density of activity (ρ) tends to decrease until it reaches a critical value where the transition may occur, and localized excavated buds may appear because of amplification processes.

To test the validity of our scenario, we have used a multi-agent model (see *Materials and Methods* and Fig. S3 of the *SI Appendix*) based on crowding along the nest perimeter and amplification processes (previous digging increases the probability of digging at the same place). The results of our simulations demonstrate that with such digging rules, a morphological transition can occur during the nest growth (Fig. 3*A* and *C* and Table 2). Simulation-generated patterns for both group sizes show a morphological transition in agreement with experimental values (simulation values: 300 ants: $\omega_1 = 0.53 \pm 0.00$, $\omega_2 = 3.17 \pm 0.51$, $n = 30$; 50 ants: $\omega_1 = 0.59 \pm 0.01$, $\omega_2 = 1.66 \pm 0.41$, $n = 30$) (Table 2). The fact that neither behavioral changes nor environmental heterogeneities are implemented in our model strongly suggests that the shape transition is due to interplay between the geometry of the nest and the global digging activity. Moreover, the model shows that, in the range of our experimental data, no morphological transition occurs in the case of a linear digging dynamics. The nest is weakly heterogeneously dug during the overall simulation ($\omega = 0.93$ during the whole excavation) (Fig. 3*B* and *C*). A nonlinear dynamic seems to be required to observe the morphological transition we describe here, as it may strongly reinforce the variation of ρ through time. As a first step, it may stabilize the isotropic growth during the first stage, as crowding is maintained by the accelerating dynamics. In a second step, it may drastically accelerate the decreasing of ρ: When the digging rate decreases, the nest becomes ramified.

Discussion

Nest digging in ants presents a morphological transition between two distinct growth stages, this phenomenon being controlled by the dynamics of digging ants' density. Our results show that different patterns may emerge even in a homogeneous environment and without behavioral changes, only as by-products of the digging process.

Our theoretical and experimental results explain the patterns of ants' nests observed under rocks, which are dug in almost 2D-conditions, and that share shapes similar to those described here. Moreover, several field studies on ants (9, 20, 21) and termites (22) have described flat, horizontal chambers that are rounded and may become lobed as they are enlarged.

Previous works (23) have shown that the relationship between colony size and nest volume could be explained without an explicit measure of the nest volume. By considering a heterogeneous distribution of ants in the nest (12), coupled to our algorithm based on
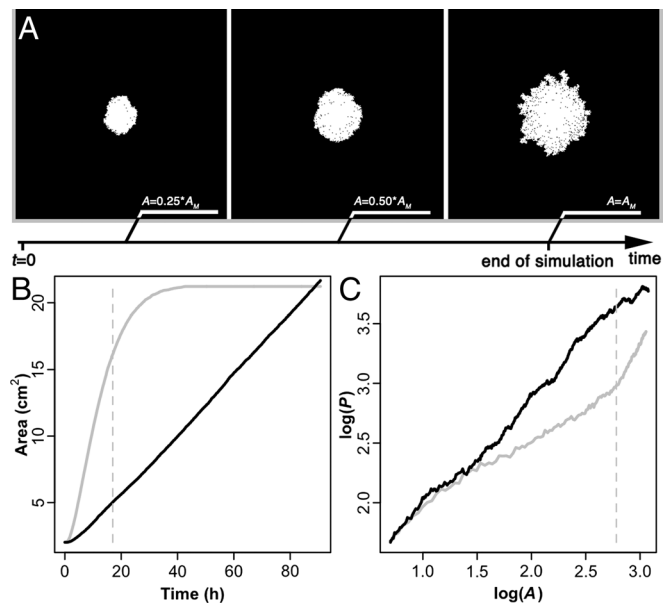
Fig. 3. Nest-digging simulations reproduce the morphological transition. (*A–C*) Results of the simulations with 50 ants ($A_{M50} = 20.18$ cm^2, $K = 50$, $\xi = 0.1\%$, $\nu = 0.05$), each condition being represented by a given color: nonlinear dynamics condition in gray (experimental digging dynamics: $\theta_{50} = 0.38$); linear dynamics condition in black (linear digging rate: $\sigma = 0.0037$). (*A*) Nest morphology at different times ($A = 0.25A_M$; $A = 0.5A_M$; $A = A_M$) for the nonlinear dynamics condition. Dug area is represented in white. (*B* and *C*) Morphological transition for nonlinear dynamics condition is represented in gray dashed lines. (*B*) Nest area (A) against time. (*C*) Logarithm of the perimeter ($log(P)$) versus logarithm of the area ($log(A)$) (nonlinear dynamics condition: $\omega_1 = 0.57$, $\omega_2 = 1.73$; linear dynamics condition: $\omega = 0.93$).

Table 2. Comparison between experimental and simulations results for both group sizes (300 and 50 ants)

Parameter	Mean $\pm$ SD (number of replicates)			
	300 ants (exp.)	300 ants (sim.)	50 ants (exp.)	50 ants (sim.)
ω_1	0.5 ± 0.03 (29)	0.53 ± 0.00 (30)	0.56 ± 0.05 (12)	0.59 ± 0.01 (30)
ω_2	1.84 ± 0.83 (29)	3.17 ± 0.51 (30)	1.55 ± 0.62 (12)	1.66 ± 0.41 (30)
A_{TRA}	49.92 ± 23.11 (29)	69.10 ± 1.18 (30)	12.60 ± 6.35 (12)	16.14 ± 1.19 (30)
ρ_{TRA}	0.038 ± 0.022 (29)	0.015 ± 0.002 (30)	0.041 ± 0.045 (12)	0.031 ± 0.010 (30)

Experimental results (exp.) are those of experiments with a morphological transition. Simulation results (sim.) are those of nonlinear dynamics condition ($A_{M\,300} = 75.18$ cm^2, $A_{M\,50} = 20.18$ cm^2, $\theta_{300} = 1.08$, $\theta_{50} = 0.38$, $K = 50$, $\xi = 0.1\%$, $\nu = 0.05$).

nest-digging activity, one may reproduce the succession of chambers (high-activity period) and tunnels (residual activity before global shutdown). This framework may conciliate the regulation of nest volume and the diversity of nest structures, as suggested by the strong relationship between A_{TRA} and A_M.

In addition, our 2D model can be easily extended to a three-dimensional (3D) model, the perimeter and area of the 2D nest becoming surface and volume of the 3D nest respectively. From our model, one can expect the excavation of spherical chambers under high digging rates that may later become ramified. However, the scenario, developed in homogeneous conditions, has to be completed with several environmental parameters. For instance, one unavoidable parameter is gravity, to which ants are known to respond by digging more frequently towards the bottom of a vertical setup (24). It has been shown that the coupling between amplification mechanisms modulated by the group size and such environmental templates may lead to very different patterns or dynamics (10, 15, 23, 25). This template effect of gravity may account for the formation of ellipsoidal chambers or of vertical tunnels (7, 9, 12, 20).

To conclude, the morphological transition described here corresponds to a branching process in which instabilities along a growth interface (i.e., the nest perimeter) lead to the formation of branched patterns (i.e. lateral galleries). Our results show that the characteristics and the occurrence of transitions depend on the group size. In social insects, such transitions have been reported for trail foraging: Small ant colonies forage in a disorganized manner, with a transition to organized pheromone-based foraging in larger colonies (26–28). Other examples are reported for gregarious insects where the density of individuals controls the emergence of aggregation patterns (29–31) or for fish, where the number of individuals affects collective decision making (32). Such morphological transitions between two stages of growth have already been described in several chemical [electrochemical deposition (33), combustion (34)], physical [viscous fingering in Hele–Shaw cells (35)], and biological [coral (36) or bacteria community (37) growth, wound healing (38), or collective migration (39)] systems.

Concerning social animals, different examples reported in the literature strongly suggest that shape transitions are not restricted to the digging of social insects. Army ants start their foraging raids by forming a swarm that sweeps the neighborhood of their bivouac. This pattern later shifts towards a small number of well-marked chemical trails (40). Gregarious larvae of bark beetles (*Dendroctonus* sp) feed side by side on the inner bark, digging a 2D feeding chamber that becomes ramified (41, 42). We postulate that such shape transition could be observed in many other group-living species. Based on our model assumption, these transitions are independent of the species and its specificities. Indeed, shape transitions can occur in any species that exhibits group activities that are based on mimetic behavior and that lead to spatial competition and exhaustion of the resources. Our scenario, based on digging ants' density, provides a new explanatory framework to account for the shift in growth stages and for the emergence of branched patterns that are widely spread in biological systems and in animal societies.

Materials and Methods

Ant Biology. *L. niger* is a common monogynous and monomorphic Palaearctic ant species whose colony size may vary from thousands to tens of thousands of individuals. Workers are characterized by age polyethism (43), in which younger ants are brood tenders and may become foragers as they grow older. *L. niger* is an opportunistic species that can feed on living or dead insects (44), but its main food consists of aphids, honeydew (45), and, occasionally, extrafloral nectaries (46). Some nests may be found under plate rocks, but most of them are dug in the soil and can be easily located by the soil crater(s) or mound(s) surrounding their entrance(s). The nest structure consists mainly of two fundamental building blocks), (i.e. chambers and tunnels), whereas the volume of the nest is correlated to the colony size (8). Colonies of *L. niger* species were reared into laboratory conditions at a temperature of 20 °C. Colonies were fed with water–sugar solution (1M) and freshly killed mealworms (*Tenebrio molitor*). Groups of 50 or 300 workers (no brood, no queen) were randomly selected from 11 mother colonies. These groups were not fed during the whole experiment to prevent the ants from being engaged in tasks other than digging.

Digging Setup. The setup was a dark box containing a horizontal digging area: two glass plates (42×42 cm), between which was placed a 2-mm high layer of wet Brusselean sand (15% of water). Groups of 300 ($n = 33$) or 50 ($n = 20$) ants were placed in a Petri dish, which was connected with the top center of the digging area by a tunnel with a radius $r = 5.5$ mm. This setup is considered 2D-effective, as ants dig the sand layer over its entire thickness and move only into horizontal directions. Such experimental digging conditions allow dynamical observations of the nest (13, 14). Two-dimensional nest patterns also exist in the field, especially under plate rocks, because of the strong thigmotactism shown by ants (25). All the experiments were carried out between November 2005 and April 2007, with each experiment ending after 90 h.

Experimental Measures. Snapshots of the digging area were taken from below every 10 minutes under red light (47). Pictures have been automatically segmented to measure both the area and perimeter of the nest. All the statistical analyses were made by using R software (version 2.8.0) (48).

Analysis of Nest Shape and Morphological Transition. The relationship between area (A) and perimeter (P) of the nest has been used to characterize changes of the nest pattern and the occurrence of the morphological transition. This relationship describes the roughness of the nest cavity with the equation $P = \mu A^\omega$, the parameters' values being, in the case of a circle, $\mu = 2\sqrt{\pi}$ and $\omega = 0.5$. The experimental value of ω is estimated by calculating the slope of the regression line of $log(P) = \omega log(A)$. When ω is close to this lowest theoretical value, the nest border is as smooth as that of a disc. This parameter value will increase over time as soon as "buds" appear along the nest wall and make the nest cavity rough after the first transition. The transition point is characterized by a steep increase in the aforementioned relationship.

Statistical Characterization of the Transition Point. The transition point has been characterized for each experiment by using a linear regression method (49) that splits a global set of values (of size N) into two subsets (of sizes n_1 and $n_2 = N - n_1$), calculates their linear regression parameters, and computes a global standard deviation. This method is based on the following equation:

$$y = a_0 + b_0 x + a_1 \text{STAGE} + b_1 \text{STAGE}\,x, \qquad \text{[3]}$$

where a_0 and b_0 are the linear regression line parameters of the first subset (before transition) and $a_0 + a_1 = a_2$ and $b_0 + b_1 = b_2$ are those of the second subset (after transition). STAGE is a binary variable whose value is 0 and 1 for points of the first and second subsets respectively. The first standard deviation value is calculated with $n_1 = 1$. For each subsequent calculation step (as long as $n_1 < N - 1$), the size of n_1 is increased by adding the next point (in chronological order), this value being removed from the n_2 subset. The transition point is the point at which the global standard deviation is the lowest.

The relevance of the transition point is tested with an F-test that compares the r squared of the first subset with that of the global set of values.

Comparison Between 50- and 300-Ant Experiments. All measured parameters (α, β, ω, ρ) from each set of experimental conditions have been compared by using Mann–Whitney rank sum test. Area (A) has been normalized before comparison. A_{NORM} is the area dug per ant $A_{\text{NORM}} = \frac{A_{300}}{300} = \frac{A_{50}}{50}$.

Simulations. Simulations have been made by using lattices of square cells (600×600) standing for the digging setup. The correspondence between physical and theoretical values has been determined by using experimental measures (see *SI Appendix*). We determine that a nest cell has an area of $A_{cell} = 0.07$ mm^2 and that an ant is four cells wide ($L.\ niger$ head's width is ≈1 mm). The duration of a time step is 1 minute, and a simulation lasts 5,400 time steps (which corresponds to the 90-h duration of the experiments). Each simulation starts with an initial circular area A_0 (radius $= 20$ cells, which corresponds to the access hole of the experimental setup); (see Fig. S3 of the *SI Appendix*).

The experimental nonlinear digging dynamic is a by-product of the competition between positive feedback loops amplifying digging and negative loops consisting of aggregation. The calculation of the digging rate takes into account a saturation process (A_M) and an excavation process limited by the crowding close to the digging zone. This crowding zone is approximated by the perimeter P of a circle of surface A as $P \simeq A^{0.5}$ (see *SI Text* and Fig. S1 of the *SI Appendix*). The area excavated per time step is therefore

$$\tau = \theta A^{0.5}\left(1 - \frac{A}{A_M}\right) \cdot \Delta t, \qquad \textbf{[4]}$$

where A_M is the nest final area and θ is a characteristic parameter of the digging rate. The resulting digging dynamics are well fitted by Eq. 1 (Fig. S2 of the *SI Appendix*). The mean values of θ were then estimated with experimental dynamics: $\theta_{50} = 0.38 \pm 0.43$ ($n = 12$); $\theta_{300} = 1.08 \pm 0.39$ ($n = 29$). The number of sand pellets that are excavated at each time step (N_{pel}) is calculated as

$$N_{pel} = \frac{\tau}{A_{cell}}. \qquad \textbf{[5]}$$

We also studied how the level of nonlinearity of the excavation process may act upon the nest morphogenesis by making simulations with a linear digging dynamic defined as

$$\tau = \sigma \cdot \Delta t, \qquad \textbf{[6]}$$

with $\sigma = \frac{A_M}{total\ number\ of\ time\ steps}$, which gives $\sigma_{300} = 0.0139$ and $\sigma_{50} = 0.0037$.

To be dug, a cell must have at least one of its eight nearest neighboring cells already dug, and a cell must be reachable by an ant (taking an ant head's width into account). At each time step, the list of reachable cells (of length N_{reach}) is updated, and the number of excavated pellets at this time step (N_{pel}) is calculated (Eq. 4 or 6, depending on the chosen digging dynamics).

Then, for each of N_{pel} pellet excavations, the probability of each cell i to be dug is computed as follows:

$$p_{dig\,i} = \frac{C_i}{\sum_{i=0}^{N_{reach}} C_i} \qquad \textbf{[7]}$$

$$C_i = \frac{x^2}{x^2 + K^2} + \xi, \qquad \textbf{[8]}$$

where x is the total quantity of pheromone already present in the eight nearest neighboring cells, K is the number of pheromone units needed to get a response of 50%, and ξ is the intrinsic probability of the cell to be dug (i.e., when $x = 0$). One of these cells is randomly chosen and dug according to its value of p_{dig} and then is filled with 100 units of pheromones. At the end of the time step, a given fraction of pheromone (ν) has evaporated while nest area and perimeter are computed. Then the simulation enters the following time step.

1. Hansell MH (2005) *Animal Architecture* eds Willmer P, Norman D (Oxford Univ Press, Oxford).
2. Turner SJ (2000) *The Extended Organism. The Physiology of Animal-Built Structures* ed Press HU (Harvard edition World, Cambridge, MA), p 235.
3. Kleineidam C, Roces F (2000) Carbon dioxide concentrations and nest ventilation in nests of the leaf-cutting ant *Atta vollenweideri*. *Insect Soc* 47:241–248.
4. Buhl J, et al. (2004) Efficiency and robustness in ant networks of galleries. *Eur Phys J B* 42:123–129.
5. Buhl J, Gautrais J, Deneubourg JL, Theraulaz G (2004) Nest excavation in ants: Group size effects on the size and structure of tunneling networks. *Naturwissenschaften* 91:602–606.
6. Halley JD, Burd M, Wells S (2005) Excavation and architecture of Argentine ant nests. *Insect Soc* 52:350–356.
7. Mikheyev AS, Tschinkel WR (2004) Nest architecture of the ant *Formica pallidefulva*: structure, costs and rules of excavation. *Insect Soc* 51:30–36.
8. Rasse P, Deneubourg JL (2001) Dynamics of nest excavation and nest size regulation of *Lasius niger* (Hymenoptera: Formicidae). *J Insect Behav* 14:433–449.
9. Tschinkel WR (2005) The nest architecture of the ant, *Camponotus socius. J Insect Sci* 5:9.
10. Bonabeau É, et al. (1998) A model for the emergence of pillars, walls and royal chambers in termite nests. *Philos Trans R Soc London Ser B* 353:1561–1576.
11. Theraulaz G, Bonabeau É (1995) Coordination in distributed building. *Science* 269:686–688.
12. Cassill DL, Tschinkel WR, Vinson SB (2002) Nest complexity, group size and brood rearing in the fire ant, *Solenopsis invicta. Insect Soc* 49:158–163.
13. Sudd JH (1971) The effect of tunnel depth and of working in pairs on the speed of excavation in ants (*Formica lemani* Bondroit). *Anim Behav* 19:677–686.
14. Sudd JH (1970) The response of isolated digging worker ants *Formica lemani* Bondroit and *Lasius niger* (L.) to tunnels. *Insect Soc* 49:261–272.
15. Camazine S, et al. (2001) *Self-Organization in Biological Systems*, Princeton Studies in Complexity, eds Anderson PW, Epstein JM, Foley DK, Levin SA, Nowak MA (Princeton Univ Press, Princeton), p 538.
16. Sumpter DJT (2006) Review. the principles of collective animal behaviour. *Philos Trans R Soc London Ser B* 361:5–22.
17. Buhl J, Deneubourg JL, Grimal A, Theraulaz G (2005) Self-organized digging activity in ant colonies. *Behav Ecol Sociobiol* 58:9–17.
18. Depickère S, Fresneau D, Deneubourg JL (2004) Dynamics of aggregation in *Lasius niger* (Formicidae): Influence of polyethism. *Insect Soc* 51:81–90.
19. Hangartner W (1969) Carbon dioxide, a releaser for digging behavior in *Solenopsis geminata* (hymenoptera: Formicidae). *Psyche* 76:58–67.
20. Tschinkel WR (2004) The nest architecture of the florida harvester ant, *Pogonomyrmex badius. J Insect Sci* 4:19.
21. Tschinkel WR (2003) Subterranean ant nests: Trace fossils past and future? *Palaeogeogr Palaeoclimatol Palaeoecol* 192:321–333.
22. Grassé PP (1984) *Termitologia*: *Fondation des Sociétés Construction* (Masson, Paris) Vol 2 (in French).
23. Deneubourg JL, Franks NR (1995) Collective control without explicit coding: The case of communal nest excavation. *J Insect Behav* 8:417–432.
24. Sudd JH (1972) The response of digging ants to gravity. *Insect Soc* 3:243–250.
25. Dussutour A, Deneubourg JL, Fourcassié V (2005) Amplification of individual preferences in a social context: The case of wall-following in ants. *Proc R Soc London Ser B* 272:705–714.
26. Beekman M, Sumpter DJT, Ratnieks FLW (2001) Phase transition between disordered and ordered foraging in Pharaohs' ants. *Proc Natl Acad Sci USA* 98:9703–9706.
27. Detrain C, Deneubourg JL, Goss S, Quinet Y (1991) Dynamics of collective exploration in the ant *Pheidole pallidula. Psyche* 98:21–32.
28. Couzin I, Franks NR (2003) Self-organised lane formation and optimised traffic flow in army ants. *Proc R Soc London Ser B* 270:139–146.
29. Theraulaz G, et al. (2002) Spatial patterns in ant colonies. *Proc Natl Acad Sci USA* 99:9645–9649.
30. Deneubourg JL, Gregoire JC, Le Fort E (1990) Kinetics of the larval gregarious behavior in the bark beetle *Dendroctonus micans* (Coleoptera: Scolytidae). *J Insect Behav* 3:169–182.
31. Sempo G, Canonge S, Detrain C, Deneubourg JL (2009) Complex dynamics based on a quorum: Decision-making process by cockroaches in a patchy environment. *Ethology*, 10.1111/j.1439-0310.2009.01699.x.
32. Couzin I, Krause J, Franks NR, Levin SA (2005) Effective leadership and decision-making in animal groups on the move. *Nature* 433:513–516.
33. Zik O, Moses E (1996) Electrodeposition: The role of concentration in the phase diagram and the hecker transition. *Phys Rev E* 53:1760–1764.
34. Zik O, Olami Z, Moses E (1998) Fingering instability in combustion. *Phys Rev Lett* 81:3868–3871.
35. Saffman PG, Taylor G (1958) The penetration of a fluid into a porous medium or hele-shaw cell containing a more viscous liquid. *Proc R Soc London Ser A* 245:312–329.
36. Merks R, Hoekstra A, Kaandorp J, Sloot P (2003) Models of coral growth: Spontaneous branching, compactification and the Laplacian growth assumption. *J Theor Biol* 224:153–166.
37. Ben-Jacob E (2008) Social behavior of bacteria: From physics to complex organization. *Eur Phys J B* 65:315–322.
38. Omelchenko T, Vasiliev J, Gelfand I, Feder H, Bonder E (2003) Rho-dependent formation of epithelial "leader" cells during wound healing. *Proc Natl Acad Sci USA* 100:10788–10793.
39. Gueron S, Levin SA (1993) Self-organization of front patterns in large wildebeest herds. *J Theor Biol* 165:541–552.
40. Gotwald WH, Jr (1995) *Army Ants* (Cornell University, Ithaca, NY).
41. Grégoire JC, Merlin J (1984) *Dendroctonus micans*: The evolution of a brood system. In *Proceedings of the EEC Seminar on the Biological Control of Bark Beetles (Dendroctonus micans), Brussels, 3-4/10/1984*, eds Grégoire JC, Pasteels JM, (Commission of the European Community, Brussels), pp 80–86.
42. Grégoire JC (1988) *The Greater European Spruce Beetle*, ed Berryman A (Plenum, New York), pp 455–478.
43. Lenoir A, Ataya H (1983) Polyethism and distribution of activity levels in Lasius niger ant I. *Z Tierpsychol* 63:213–232 (in French).
44. Pontin AJ (1961) The prey of Lasius niger (l.) and Lasius flavus (f.) (hym., formicidae). *Entomol Monogr Mag* 97:135–137.
45. Pontin A (1958) A preliminary note on the eating of aphids by ants of the genus *Lasius niger* (hym., formicidae). *Entomol Monogr Mag* 94:9–11.
46. Sakata H, Hashimoto Y (2000) Should aphids attract or repel ants? Effect of rival aphids and extrafloral nectaries on ant-aphid interactions. *Popul Ecol* 42:171–178.
47. Depickère S, Fresneau D, Deneubourg JL (2004) The influence of red light on the aggregation of two castes of the ant, *Lasius niger. J Insect Physiol* 50:629–635.
48. Ihaka R, Gentleman R (1996) R: A language for data analysis and graphics. *J Comput Graph Stat* 5:299–314.
49. Draper NR, Smith H (1981) *Applied Regression Analysis* (Wiley, New York) 2nd Ed.